

Low Overhead Beam Alignment for Mobile Millimeter Channel Based on Continuous-Time Prediction

Huang-Chou Lin and Kuang-Hao (Stanley) Liu, *Member, IEEE*

Abstract

In millimeter-wave (mmWave) communications, directional transmission based on beamforming is important to compensate for high pathloss. To maintain the desired direction transmission gain, beam scanning that involves the transmitter sending the pilot signal over all available beam directions to find the optimal beam is often considered. Alternatively, beam tracking using partial beams can save the beam training overhead through algorithms such as statistical analysis models and kalman filter (KF). Unfortunately, existing beam tracking solutions are limited to a fixed beam variation pattern. In this work, we propose a beam alignment scheme called adaptive online beam alignment (AOBA), which aims to reduce training overhead and achieve accurate beam alignment for any movement profile. The proposed AOBA periodically performs beam tracking using a small amount but carefully selected candidate beams and switches to beam scanning using all available beams based on a given switching rule. During the interval without the pilot signal, the optimal beam at an arbitrary time instant is predicted with the aid of the recently proposed ordinary differential equation (ODE)-long short-term memory (LSTM) model. Extensive simulations are conducted to evaluate the performance of the proposed AOBA in comparison with several existing beam alignment schemes.

I. INTRODUCTION

Millimeter Wave (mmWave) communication is a promising technique to fulfill the ever-growing demand for high data rate transmission [1]. It has been employed to develop emerging 5G applications. However, mmWave channels suffer high propagation loss and blockage effect that make it difficult to maintain seamless mmWave connectivity [2]. Fortunately, the small wavelength of mmWave allows densely packed antenna elements in a small form factor. Hence, the array antenna consisted of many elements has been commonly used in mmWave communication to achieve directional beamforming [3].

In general, high beamforming gain requires more antenna elements to synthesize narrow beams with great array gain. Meanwhile, the alignment of highly directional and narrow beams is essential to maintain the desired beamforming gain. A common solution to find the best beam direction is to transmit the pilot signal in all the possible

S.-Y. Huang is with the Institute of Computer and Communication Engineering, National Cheng Kung University, Tainan, Taiwan 701. E-mail: qq36091017@gs.ncku.edu.tw

K.-H. Liu is with the Institute of Communications Engineering, National Tsing Hua University, Hsinchu, Taiwan 300044. E-mail: khliu@ee.nthu.edu.tw

directions, known as beam scanning or sweeping [4]. When the optimal beam direction changes frequently, e.g., in mobile applications, beam scanning causes dramatic training overhead. Two approaches have been studied to maintain high directivity with low training overhead for mmWave communication, namely beam tracking [5] and beam prediction [6]–[10]. Beam tracking attempts to find the optimal beam by tracking the variations of the time-varying channel gains and angles. This can be done through estimation algorithms such as Kalman filter (KF) to estimate the channel state for each slot between two consecutive pilot transmissions [11]–[13]. Thanks to periodic pilot transmissions, the training overhead of beam tracking can be greatly reduced compared to beam scanning. Further reduction is possible if some candidate beams are selected to send the pilot signal as in [14], [15]. Similarly, beam prediction also finds the optimal beam based on periodically received pilot signal. Unlike beam tracking, beam prediction does not explicitly estimate the variations of channel gains and angles but only focus on the forecast of the optimal beam on a per slot basis. Some existing work treats beam prediction as a time-series forecasting problem that can be addressed using a variety of statistical and machine learning (ML) based methods (see [16] and the references therein).

While some initial works have shown the success of ML based methods in carrying out beam prediction [7]–[10], they all make the prediction based on the pilot signal transmitted over all beams, resulting in high training overhead. As a result, existing beam prediction approaches are difficult to be implemented in practice. To bridge this gap, this work focus on reducing the beam training overhead of beam prediction for mmWave. Specifically, we propose to make prediction using partial beams, which we call the probing beams. Clearly, the prediction accuracy is heavily dependent on the subset of probing beams and it degrades with time. To overcome the former, we study three training beam selection strategies and the latter is addressed by invoking beam scanning under two given conditions. In this way, we are able to maintain accurate beam alignment by alternating different operation modes, namely, beam scanning, beam tracking, and beam prediction while keeping the training overhead as low as possible.

The remainder of this paper is organized as follows. Sec. II explain the system model and problem under study. The proposed approaches to reduce the beam training overhead for mmWave are presented in Sec. III, including the training beam selection schemes, the beam prediction method, and the switching rule between different beam alignment modes. Simulation results are shown in Sec. IV followed by concluding remarks given in Sec. V.

II. SYSTEM MODEL AND PROBLEM DESCRIPTION

Consider a mmWave user equipment (UE) served by a base station (BS). The BS has M antennas in uniform linear array (ULA) and the UE has a single antenna. We focus on the analog beamforming where each BS antenna element is connected to a phase shifter and all the phase shifters are connected to a single RF chain. In practice, the phase shifters have finite resolutions. In this work, we assume each phase shifter can vary its phase in Q quantization levels.

Since the mmWave channel is sparse in nature, we adopt a geometric channel model to characterize the channel between the BS and the UE at time t as [6], [9]

$$\mathbf{H}_t = \sum_{l=1}^L \alpha_{t,l} \mathbf{a}(\phi_{t,l}) \quad (1)$$

where L is the number of paths, $\alpha_{t,l}$ and $\phi_{t,l}$ are the path gain and angle of departure (AoD), respectively, of the l th path at time t , and $\mathbf{a}(\phi_{t,l}) \in \mathbb{C}^M$ denotes the steering vector of the ULA at the BS given by $\mathbf{a}(\phi_{t,l}) = 1/\sqrt{M}[1, e^{j2\pi d \sin(\phi_{t,l})/\lambda}, \dots, e^{j(M-1)2\pi d \sin(\phi_{t,l})/\lambda}]^T$ with d and λ being the antenna spacing and the wavelength, respectively. Let $s \in \mathbb{C}$ denote the transmit signal from the BS, which uses the analog beamforming vector denoted as $\mathbf{f} \in \mathbb{C}^M$. At time t , the received signal at the UE is given by

$$\mathbf{y}_t^{(q)} = \mathbf{H}_t^T \mathbf{f}_q s + \mathbf{z}_t \quad (2)$$

where $|s| = 1$ and \mathbf{z}_t is the additive white Gaussian noise (AWGN) with zero mean and variance σ^2 . Here, \mathbf{f}_q is the analog beamforming vector selected from a codebook based on the discrete Fourier transform (DFT). The codebook contains Q codewords with the q -th codeword given by [9], [10]

$$\mathbf{f}_q = \sqrt{\frac{1}{M}}[1, e^{j2\pi\theta_q}, \dots, e^{j2\pi(M-1)\theta_q}] \quad (3)$$

where $\theta_q = q/Q$.

Due to the movement of the UE, the AoD of the BS-UE channel changes with time and thus the BS needs to update its beamforming vector to align with the channel AoD. This can be achieved by selecting the optimal beamforming vector from the codebook that maximizes the beamforming gain defined as $G_t = |\mathbf{H}_t^T \mathbf{f}_q|^2$. Thus, the best beam index q_t^* at time t is given by

$$q^*(t) = \underset{q \in \{1, 2, \dots, Q\}}{\operatorname{argmax}} G_t. \quad (4)$$

While $q^*(t)$ can be found by *beam scanning*, i.e., the BS sends the pilot signal using all available beamforming vectors and the UE measures their corresponding beamforming gains, this approach induces significant training overhead and delay when Q is large. On the other hand, the DFT codebook of size Q has an angular resolution of $1/Q$. As a result, a large Q is beneficial to increase the angular resolution of the DFT codebook. One way to strike the balance between the angular resolution and beam training overhead is to keep Q large but perform beam scanning periodically instead of every time slot. Clearly, the optimal beam scanning period depends on the UE moving speed, which is not necessarily constant and thus it is difficult to optimize the beam scanning period in real time. Our remedy is to predict q_t^* for the time in the fixed beam scanning period. It is worth to mention that the BS can choose to probe a subset of available beamforming vectors instead of all available beams to further reduce the training overhead. In this case, the beam prediction accuracy is closely related to the beam subset to probe, which needs to be carefully chosen. Denote S the number of probing beams used to send the pilot signal. We refer to the case of $S < Q$ as *beam tracking* to be not confused with beam scanning using Q probing beams.

III. OVERHEAD REDUCTION WITH ADAPTIVE BEAM ALIGNMENT

To reduce overhead for mmWave beam alignment, we consider a periodic beam alignment protocol as shown in Fig. 1. The protocol alternates between two stages, namely the beam alignment stage and the beam prediction stage. In the beam alignment stage, the BS transmits the pilot signal to the UE for beam alignment. The beam alignment

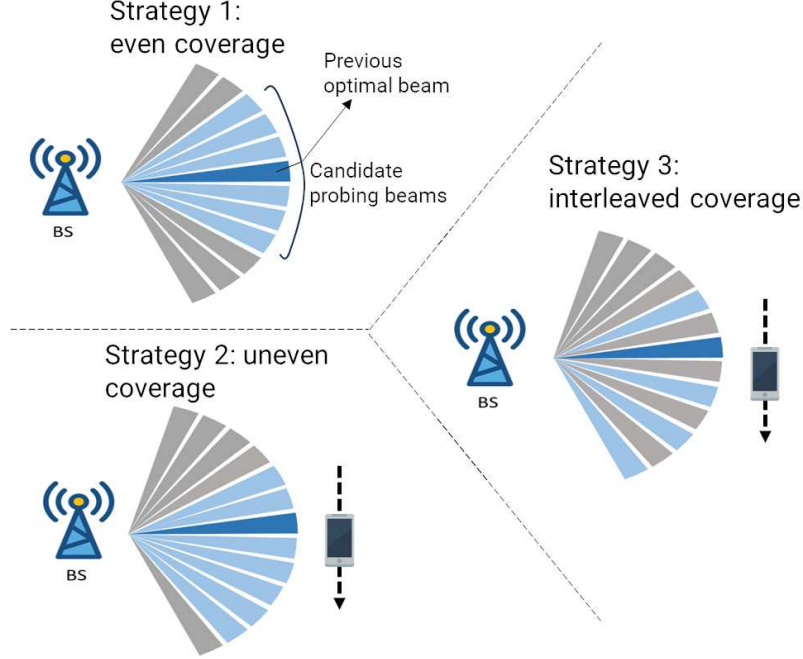


Fig. 2: Illustration of three beam selection strategies.

- Even coverage: The candidate beams are selected to cover the angular domain centered at the angle corresponding to q_{n-1}^* .
- Uneven coverage: This strategy considers the direction of the beam variation within a time window. As shown in Fig. 2, suppose the angle variation changes clockwise, we assign $|\mathcal{S}| - J_0$ for $J_0 \geq 1$ candidate beams at most to the clockwise direction including q_{n-1}^* and reserve J_0 candidate beams in the counterclockwise direction to account for potential alignment errors due to noise.
- Interleaved coverage: It is similar to the uneven coverage, except that the candidate beams are selected in an interleaved manner.

B. Beam Prediction

Our beam prediction module leverages ODE-LSTM proposed in [9], which is shown to achieve high prediction accuracy using all available beams to collect the pilot signals. When partial candidate beams are used for prediction, i.e., in the beam tracking mode, we show that ODE-LSTM still predicts the optimal beam with high accuracy. Thanks to the fewer beams used in the beam tracking mode, ODE-LSTM can be simplified that contributes to faster training and prediction speed. For completeness, we outline the key components in ODE-LSTM and refer the interested readers to [9] for details.

Fig. 3 depicts the operation procedure of the beam prediction module in the proposed AOBA. To illustrate, we assume that beam training is invoked in the n -th beam alignment stage. Given the received pilot signal vector, which is denoted as $\tilde{\mathbf{Y}}(t_n) = [\mathbf{y}_{t_n}^{(q)}]_{q \in \mathcal{S}}$, a convolutional neural network (CNN) is used to extract the preliminary feature vector denoted as $\mathbf{x}(t_n)$, which is fed into a standard long short-term memory (LSTM) cell for further feature

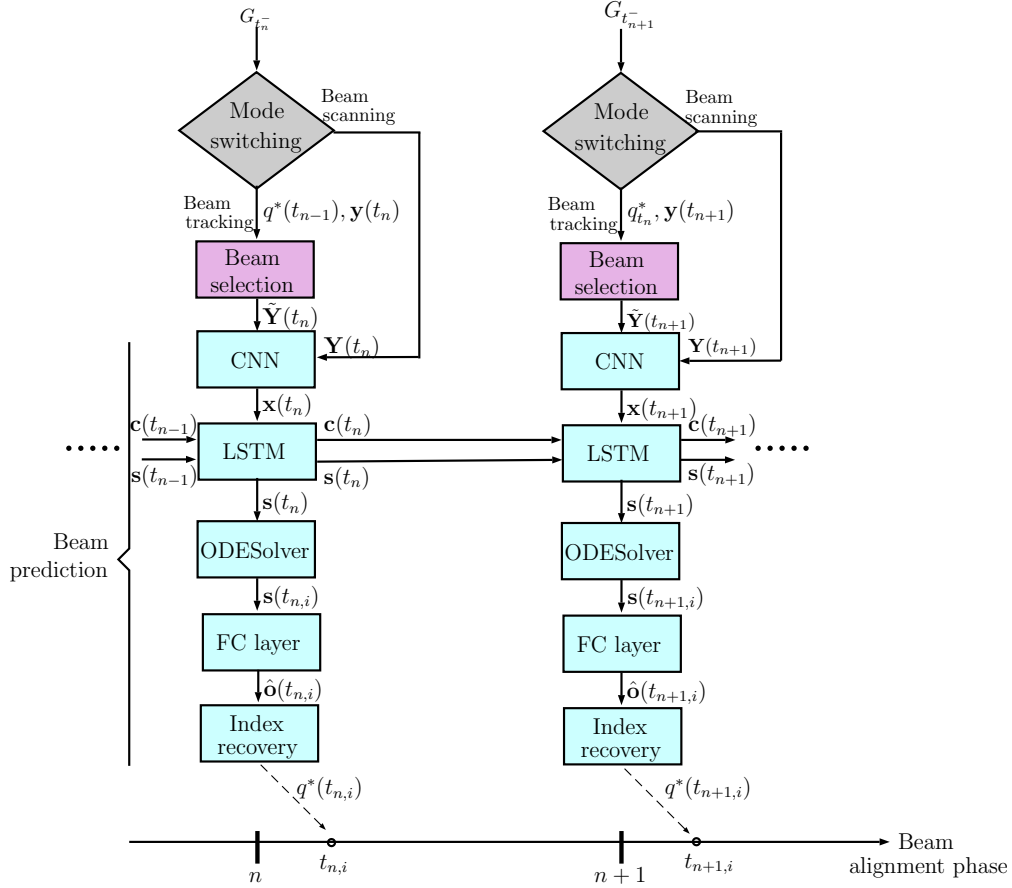


Fig. 3: The workflow of the proposed AOBA, where $t_{n,i}$ represent the i -th prediction instant between t_n and t_{n+1} .

extraction. If beam scanning is performed in the n -th beam alignment stage, the received pilot signal is denoted as $\mathbf{Y}(t_n) = [\mathbf{y}_{t_n}^{(q)}]_{q=1, \dots, Q}$. The core idea is that, when the UE moves, its channel angle variations are correlated in time. Hence, the channel information of previous time steps can be used to predict the optimal beams of the future time steps based on LSTM. In particular, the forgetting and updating mechanisms in LSTM are useful to learn the channel variations, thereby improving beam prediction accuracy. A standard LSTM cell comprises a cell state $\mathbf{c}(t_n)$, a hidden state $\mathbf{h}(t_n)$, an input feature $\mathbf{x}(t_n)$, an input gate, an output gate, and a forget gate. The cell state remembers the previous data, and the hidden state enables the LSTM to learn non-linear dynamics. The forget gate determines which information should be omitted from memory at a specific time. The input gate consists of two components: the sigmoid function responsible for determining which feature should be selected, and the other is the tanh function, which updates weights for the propagated values. Finally, the output gate is multiplied by the previous hidden state $\mathbf{s}(t_{n-1})$ and the current input $\mathbf{x}(t_n)$ to produce the output along with the new hidden state $\mathbf{h}(t_n)$ and the cell state $\mathbf{c}(t_n)$.

The standard LSTM can only provide a one-step prediction. To remedy, an ODE solver is added to capture beam variation in continuous time [9]. Since the hidden state during the prediction duration is unknown, the ODE solver learns the derivative of the hidden state function with respect to time, i.e., $ds(t)/dt$. Then by solving an initial

value problem using an ODE solver, an approximation of the unknown hidden state at an arbitrary time instant can be obtained. While the ODE solver can find the hidden state in continuous time, it can also be implemented in discrete time. For example, if the prediction duration is divided into multiple time slots, we can find the hidden state of the i -th slot in the n -th prediction stage by using the ODE solver with the output denoted as $\mathbf{s}(t_{n,i})$. Finally, a fully connection (FC) layer is employed to transform the hidden state $\mathbf{s}(t_{n,i})$ into the candidate beam set. The output of the FC layer is normalized into the probabilities through the softmax activation layer. Let $\mathbf{o}(t_{n,i}) = [o^{(1)}(t_{n,i}), o^{(2)}(t_{n,i}), \dots, o^{(|S|)}(t_{n,i})]$ the output of the activation layer where $o^{(q)}(t_{n,i})$ represents the probability of the q th beam in set \mathcal{S} being the optimal one at time $t_{n,i}$. Based on $o^{(q)}(t_{n,i})$, the beam with the maximal probability is selected as the optimal beam with the index given by

$$\hat{q}^*(t_{n,i}) = \operatorname{argmax}_{q \in \mathcal{S}} o^{(q)}(t_{n,i}). \quad (5)$$

Notice that the beam index in (5) may differ from the actual beam index when $S < Q$. Fortunately, the true beam index can be easily recovered based on the knowledge of the candidate beam set \mathcal{S} .

C. Mode Switching

One limitation of beam prediction is that the prediction accuracy degrades with time. This problem can be addressed by performing periodic beam training to get a timely update of the beam variation pattern. As mentioned, we consider two operation modes in the beam training stage, namely the beam scanning using all available beams and beam tracking using partially selected candidate beams. By default, beam tracking is used for its low overhead. To switch from beam tracking mode to beam scanning mode, we propose two switching rules. To ease our explanation, define $\zeta \in \{\text{True}, \text{False}\}$ a boolean variable. When ζ is `True`, mode switching occurs and ζ is `False` otherwise.

- Periodic switching: The beam scanning and beam tracking is alternately performed in a fixed period denoted as T_s . The corresponding switching rule can be expressed as

$$\zeta = \begin{cases} \text{True}, & \text{if } t_n \bmod T_s = 0, \\ \text{False}, & \text{otherwise.} \end{cases} \quad (6)$$

- Adaptive switching: The operation mode is switched from beam tracking to beam scanning according to the quality of the latest prediction result, which can be measured by the beamforming gain $G_{t_n^-}$, where t_n^- represents the last prediction instant in the n -th prediction duration. If $G_{t_n^-}$ is less than a prescribed threshold denoted as G_0 , it implies the prediction based on the candidate beam set \mathcal{S} is no longer sustainable and full beam scanning should be invoked. Otherwise, beam training can be used without change. Such an adaptive switching rule can be expressed as

$$\zeta = \begin{cases} \text{True}, & \text{if } G_{t_n^-} < G_0 \\ \text{False}, & \text{otherwise.} \end{cases} \quad (7)$$

Comparing these two switching rules, the periodic switching does not use any information about the previous prediction result and thus it is an open-loop mechanism. On the other hand, the adaptive switching is closed-loop

in nature because the UE needs to report the thresholding result to the BS. Despite the extra overhead due to UE feedback, the adaptive switching is more robust to diverse beam variation scenarios and bypass the difficulty of determining a proper switching period. We will compare their performance in Sec. IV.

IV. SIMULATION RESULTS

TABLE I: Layer parameters used for beam scanning and beam tracking (marked by *)

Layer	Output size	Activation
3 (2^*) \times Conv2D	$32 \times 256(*64) \times 10$	ReLU
LSTMcell	$32 \times 256(*64)$	Sigmoid,tanh
ODESolver	$32 \times 256(*64)$	tanh
FC	$32 \times 64(*11)$	Softmax

In simulation, we use DeepMIMO [17], which is a ray-tracing based channel generator to generate the mmWave channel dataset considering the outdoor scenario (O1) and the first user grid (UG1). To model the user mobility, we collect samples of different UE locations following 10,240 trajectories. Details about the mobility model, model training and validation approaches are summarized in [18]. The proposed AOBA is implemented in PyTorch with the prediction module structure listed in Table I. The simulation parameters follow those considered in [9], except that the beam alignment period T is 100 ms, which is also identical to the period of mode switching T_s . Two sets of evaluations are conducted in the following.

- Set A: The mode switching module is deactivated. This allows us to identify the efficacy of the proposed beam selection strategy along with beam prediction based on ODE-LSTM. In this case, $|\mathcal{S}| = 11$ candidate beams selected every T seconds are used to predict the optimal beams for 99 time instants with uniform intervals in T seconds.
- Set B: The mode switching module is activated. Our goal is to examine the efficacy of mode switching module by performing the complete AOBA scheme.

We evaluate various beam alignment schemes in terms of the normalized beamforming gain defined as

$$\bar{G}_t = \frac{|\mathbf{H}_t^T \mathbf{f}_{\hat{q}^*(t)}|^2}{|\mathbf{H}_t^T \mathbf{f}_{q^*(t)}|^2} \quad (8)$$

where $q^*(t)$ and $\hat{q}^*(t)$ denote the index of the true and the predicted optimal beam, respectively, at time t .

Comparison of beam selection strategies (Set A): We first compare the prediction accuracy of three candidate beam selection strategies in Fig. 4 with varied UE velocity and $J_0=2$. It can be seen that the uneven strategy and the even strategy significantly outperform the interleaved strategy. While the interleaved strategy also takes the moving direction into account, the interleaving actually magnifies the angular quantization errors of the analog beamformers. This results in a lower sampling rate of a time series that causes learning failure of LSTM. Since the uneven strategy outperforms the other two strategies, it will be used in the rest of simulations.

Comparison of beam prediction methods (Set A): We examine the prediction performance within one prediction period considering three benchmarks, namely autoregression integrated moving average (ARIMA), LSTM, and extended kalman filter (EKF). They are commonly used to carry out time-series forecasting [19], which is exactly the

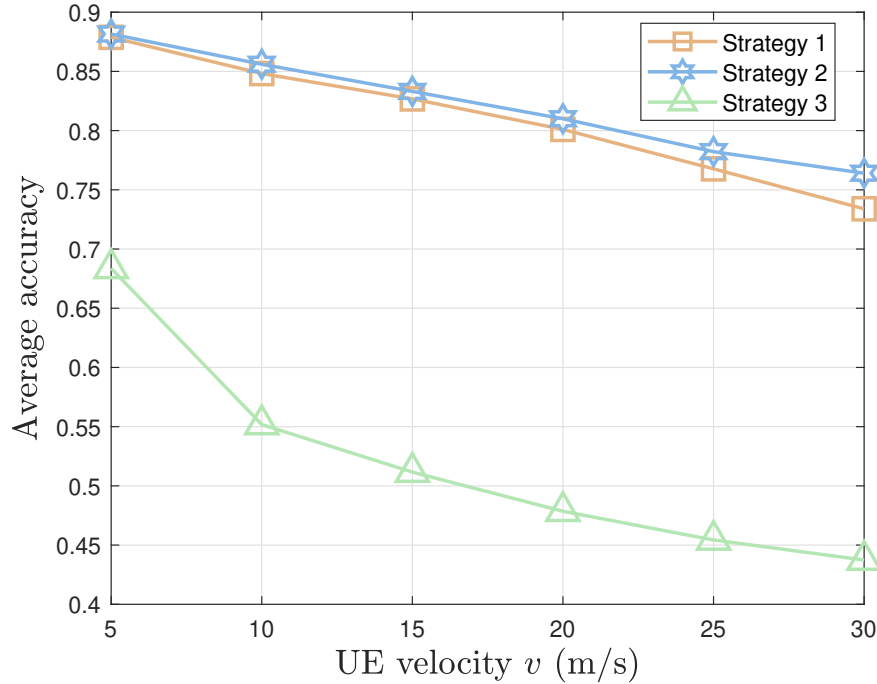


Fig. 4: Comparison of prediction accuracy of three candidate beam selection strategies versus UE velocity.

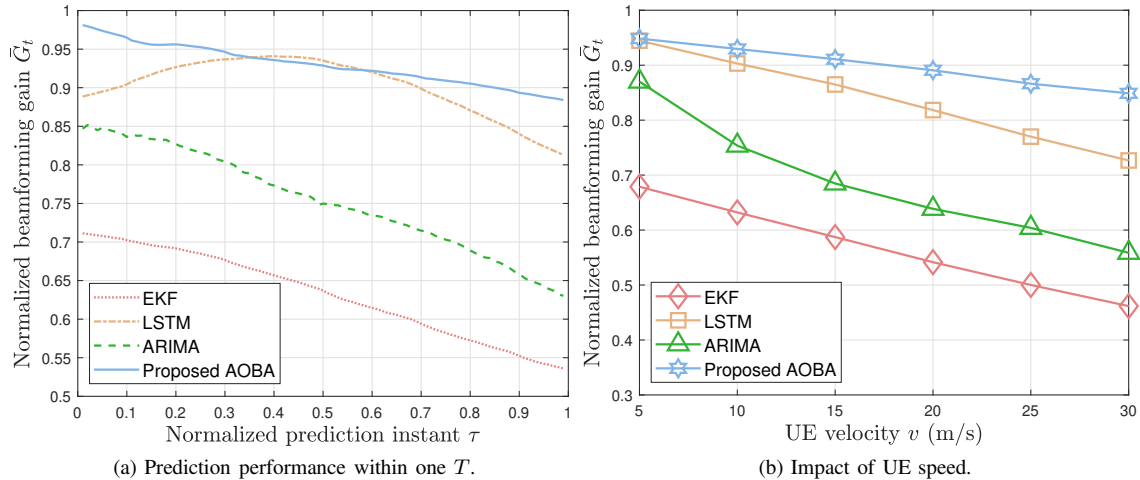


Fig. 5: Comparison of different beam prediction methods for 1-second trajectories.

same problem as beam prediction in our work. Except ARIMA that assumes linear dependence between observations, all the other methods can work for a nonlinear process. We use Python library PMDARIMA [20] to select the parameters of ARIMA, including the order of autoregression, degree of differencing, and the order of moving average. Based on the obtained parameters, ARIMA uses the true optimal beam indices of previous four beam align stages and the one of the current beam alignment stage to predict the optimal beams in T seconds. Fig. 5a shows the normalized beamforming gain in the normalized prediction instant defined as $\tau = (t_{n_i} - t_n)/T$ for $i = 1, 2, \dots, 99$ [9]. Here we fix the UE velocity $v = 10$ m/s and each trajectory lasts for 1 second. It is observed

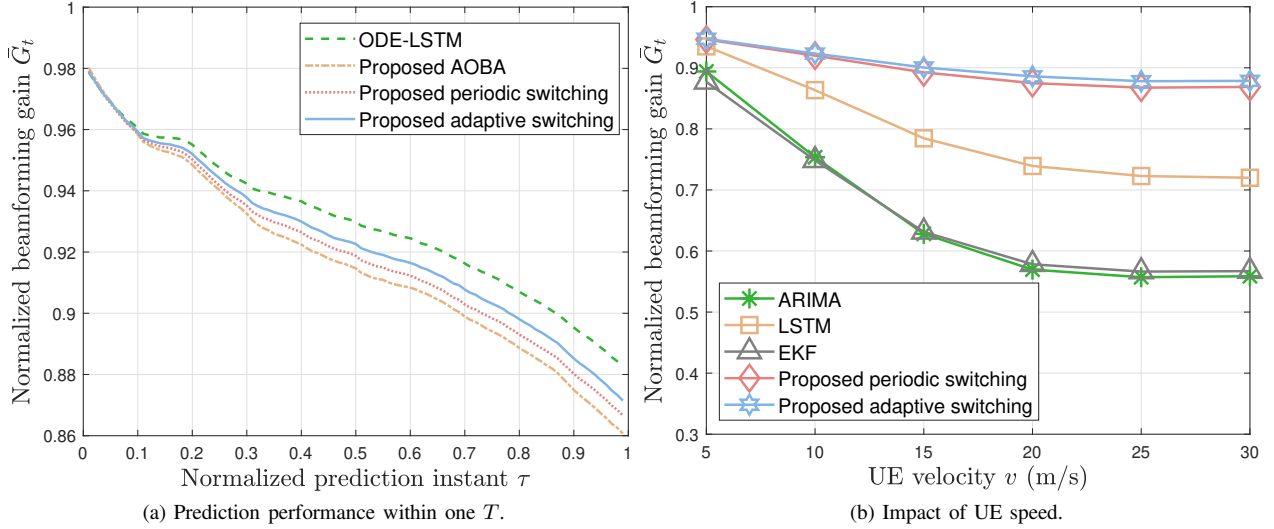


Fig. 6: Comparison of different beam prediction methods for 4-second trajectories.

that the proposed AOBA consistently offers a better accuracy than the other methods. The curve of LSTM shows a single peak because it can only deliver a one-step prediction, which tends to be the middle of T to minimize the overall performance degradation as explained in [9]. As to ARIMA, it outperforms EKF but performs much worse than LSTM and the proposed AOBA. From our experiment, ARIMA works well when it is trained to predict a single trajectory but becomes weak when it is trained to predict different trajectories. Finally, EKF performs poorly mainly because the error covariance matrix used in EKF to capture the prediction error can only be updated once per prediction period T (using the received pilot signals) that leads to accumulated errors in time.

In Fig. 5b, we show the impact of UE velocity to \bar{G}_t . At low speed, LSTM performs comparably to the proposed AOBA. As the UE velocity increases, LSTM incurs a significant degradation similar to ARIMA and EKF. It is observed that \bar{G}_t of the proposed AOBA decays slower than the competing approaches, demonstrating the robustness of AOBA to UE speed.

Comparison of mode switching rules (Set B): To evaluate the gain of mode switching, Fig. 6a shows \bar{G}_t in one prediction duration T achieved by periodic switching and adaptive switching, where the switching threshold G_0 is . Here, each trajectory is extended to 4 second. For comparison, the result of AOBA without mode switching are also included. Hence, ODE-LSTM serves as a performance upper bound because it makes prediction using the pilot signals over all available beams. The proposed AOBA with adaptive switching performs better than that with periodic switching and both outperform AOBA without mode switching. Further, Fig. 6b shows the impact of UE velocity to \bar{G}_t . Comparing with the 1-second case in Fig. 5b, AOBA with mode switching maintains nearly the same \bar{G}_t even the trajectory length increases four times. On the contrary, other competing schemes become more sensitive to velocity increase, which can be seen from the faster decay of \bar{G}_t as v increases. The above results confirm the merit of mode switching in offering high prediction accuracy for a wide range of UE velocity.

Finally, we evaluate the normalized training overhead of various prediction schemes, where the training overhead

TABLE II: Normalized training overhead

Mode switching		Enabled		Not enabled
		Periodic	Adaptive	
Speed	5 m/s	52%	52%	17%
	10 m/s		52%	
	15 m/s		53%	
	20 m/s		55%	
	25 m/s		56%	
	30 m/s		56%	

is computed as the number of beams used in sending the pilot signals normalized to the training overhead using full beam scanning every T seconds. Except AOBA, all the competing schemes, i.e., EKF, ARIMA, and LSTM do not consider mode switching and thus they fall in the same category labeled as “Not enabled” with identical training overhead in Table II for $v = 5 \sim 30$ m/s. It can be seen that the two mode switching schemes incur the same amount of training overhead at the low speed region. As the speed increases, the adaptive switching mode incurs a slightly higher overhead due to the increased frequency of invoking beam scanning. Compared with the periodic mode switching, the adaptive mode switching only has a 4% increase of training overhead at $v = 30$ m/s and it is dramatically lower than the case of beam scanning. When mode switching is not enabled, 11 out of 64 (corresponding to 17%) of beams are used per beam alignment period. Despite its low training overhead, the prediction accuracy degrades with UE velocity significantly as shown Fig. 6b.

V. CONCLUSION

Compared with state-of-art schemes including ARIMA, EKF, and LSTM, our simulation results show that AOBA successfully reduces training overhead for accurate beam alignment in a single-user mmWave communication thanks to the proposed beam selection rule with the beam variation direction taking into account. When mode switching is enabled, AOBA along with periodic mode switching performs comparably to the performance upper bound using ODE-LSTM with full beam scanning while saving about 48% of the training overhead. The adaptive mode switching incurs a slightly increased training overhead as the UE velocity increases due to more frequently invoked beam scanning. With the aid of mode switching, AOBA is more robust to UE velocity and consistently maintains the normalized beamforming gain close to 90% when the trajectory length is increased from one second to four seconds in our experiment. The results reveal that the proposed AOBA is able to achieve high beam prediction accuracy using very low training overhead that is important to mobile mmWave applications. It would be interesting to extend the current work to the multi-user beam alignment, where multiple UEs within the same BS coverage have different moving patterns that further challenges accurate beam prediction.

REFERENCES

- [1] T. S. Rappaport, S. Sun, R. Mayzus, H. Zhao, Y. Azar, K. Wang, G. N. Wong, J. K. Schulz, M. Samimi, and F. Gutierrez, “Millimeter wave mobile communications for 5G cellular: It will work!” *IEEE Access*, vol. 1, pp. 335–349, 2013.
- [2] Y. Niu, Y. Li, D. Jin, and et al, “A survey of millimeter wave communications (mmwave) for 5G: opportunities and challenges,” *Wireless Netw.*, vol. 21, p. 657–2676, Nov. 2015.
- [3] W. Roh and et al., “Millimeter-wave beamforming as an enabling technology for 5G cellular communications: theoretical feasibility and prototype results,” *IEEE Commun. Mag.*, vol. 52, no. 2, pp. 106–113, Feb. 2014.

- [4] 3GPP TS 38.214, “3rd generation partnership project; technical specification group radio access network; NR; physical layer procedures for data (release 15),” Dec. 2018.
- [5] J. Bae, S. H. Lim, J. H. Yoo, and J. W. Choi, “New beam tracking technique for millimeter wave-band communications,” arXiv:1702.00276, 2017.
- [6] S. H. Lim, S. Kim, B. Shim, and J. W. Choi, “Deep learning-based beam tracking for millimeter-wave communications under mobility,” *IEEE Trans. Commun.*, vol. 69, no. 11, pp. 7458–7469, Nov. 2021.
- [7] A. O. Kaya and H. Viswanathan, “Deep learning-based predictive beam management for 5G mmwave systems,” in *Proc. IEEE WCNC*, Mar. 2021, pp. 1–7.
- [8] T. Urakami, H. Jia, N. Chen, and M. Okada, “Individual memory driven transformer deep learning model for multi-cell massive MIMO beam prediction,” in *Proc. APSIPA ASC*, Nov. 2022, pp. 1731–1736.
- [9] K. Ma, F. Zhang, and Z. Wang, “Continuous-time mmWave beam prediction with ODE-LSTM learning architecture,” *IEEE Wireless Commun. Lett.*, vol. 12, no. 1, pp. 187–191, Jan. 2023.
- [10] W. Liu, H. Ren, C. Pan, and J. Wang, “Deep learning based beam training for extremely large-scale massive MIMO in near-field domain,” *IEEE Commun. Lett.*, vol. 27, no. 1, pp. 170–174, Jan. 2023.
- [11] V. Va, H. Vikalo, and R. W. Heath, “Beam tracking for mobile millimeter wave communication systems,” in *Proc. IEEE GlobalSIP*, Dec. 2016, pp. 743–747.
- [12] F. Liu, P. Zhao, and Z. Wang, “EKF-based beam tracking for mmWave MIMO systems,” *IEEE Commun. Lett.*, vol. 23, no. 12, pp. 2390–2393, Dec. 2019.
- [13] S. G. Larew and D. J. Love, “Adaptive beam tracking with the unscented kalman filter for millimeter wave communication,” *IEEE Signal Process. Lett.*, vol. 26, no. 11, pp. 1658–1662, Nov. 2019.
- [14] K. Ma, D. He, H. Sun, Z. Wang, and S. Chen, “Deep learning assisted calibrated beam training for millimeter-wave communication systems,” *IEEE Trans. Commun.*, vol. 69, no. 10, pp. 6706–6721, Oct. 2021.
- [15] H. Echigo, Y. Cao, M. Bouazizi, and T. Ohtsuki, “A deep learning-based low overhead beam selection in mmwave communications,” *IEEE Trans. Veh. Technol.*, vol. 70, no. 1, pp. 682–691, Jan. 2021.
- [16] M. Qurratulain Khan, A. Gaber, P. Schulz, and G. Fettweis, “Machine learning for millimeter wave and terahertz beam management: A survey and open challenges,” *IEEE Access*, vol. 11, pp. 11 880–11 902, 2023.
- [17] A. Alkhateeb, “Deep MIMO: A generic deep learning dataset for millimeterwave and massive MIMO applications,” in *Proc. ITA*, 2019, pp. 1–8.
- [18] K.-H. Liu, “Low-overhead-beam-alignment-prediction,” <https://github.com/kuanghaoliu/Low-Overhead-Beam-Alignment-Prediction>, Oct. 2023.
- [19] S. Siami-Namini, N. Tavakoli, and A. Siami Namin, “A comparison of ARIMA and LSTM in forecasting time series,” in *Proc. IEEE ICMLA*, Dec. 2018, pp. 1394–1401.
- [20] Python Software Foundation, “Pmdarima library,” <https://pypi.org/project/pmdarima/>, 2023.